Journal Pre-proof

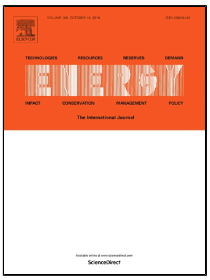

The effect of CO on the transformation of arsenic species: A quantum chemistry study

Chan Zou, Chunbo Wang, Edward Anthony

PII:	S0360-5442(19)31718-9
DOI:	https://doi.org/10.1016/j.energy.2019.116024
Article Number:	116024
Reference:	EGY 116024
To appear in:	*Energy*
Received Date:	11 March 2019
Accepted Date:	26 August 2019

Please cite this article as: Chan Zou, Chunbo Wang, Edward Anthony, The effect of CO on the transformation of arsenic species: A quantum chemistry study, *Energy* (2019), https://doi.org/10.1016/j.energy.2019.116024

This is a PDF file of an article that has undergone enhancements after acceptance, such as the addition of a cover page and metadata, and formatting for readability, but it is not yet the definitive version of record. This version will undergo additional copyediting, typesetting and review before it is published in its final form, but we are providing this version to give early visibility of the article. Please note that, during the production process, errors may be discovered which could affect the content, and all legal disclaimers that apply to the journal pertain.

© 2019 Published by Elsevier.

Energy, Volume 187, November 2019, Article number 116024
DOI: 10.1016/j.energy.2019.116024
Journal Pre-proof

The effect of CO on the transformation of arsenic species: A quantum chemistry study

Chan Zou[1], Chunbo Wang[1]*, Edward Anthony[2]

[1]Department of Energy, Power & Mechanical Engineering, North China Electric Power University, Baoding 071003, China
[2]Cranfield University, Bedford, Bedfordshire, United Kingdom
* Corresponding author: hdwchb@126.com

Abstract: To explore the effect of CO on the transformation of arsenic species, the reaction mechanism of homogeneous and heterogeneous reactions for arsenic oxides (AsO_2 and As_2O_3) with CO were investigated via density functional theory (DFT). The geometries of reactants, intermediates, transition states and products for each reaction were optimized by using the B3LYP method in conjunction with the 6-31G(d) basis set, and the single-point energy of each structure was calculated at the B2PLYP/Def2-TZVP level. Also, thermodynamic and kinetic analyses were conducted to determine the reaction process. The results showed that the homogeneous reaction of AsO_2 and CO has two channels and a transition state is found in each case. The homogeneous reaction process of As_2O_3 and CO undergoes two transition states and, finally, As_2O_3 is reduced to sub-oxides by CO. Char has a strong adsorption affinity for AsO_2 and As_2O_3 in the presence of CO, and the adsorption mode of the AsO_2 molecule on the char surface has a great influence on its reduction. The activation energy of the homogeneous reduction of As_2O_3 (75.9 kJ·mol^{-1}) is lower than the heterogeneous reduction (94.2 kJ·mol^{-1}), which suggests that As_2O_3 is more likely to react with CO in the flue gas. The calculation results revealed the mechanism for the influence of CO on arsenic behavior by density functional theory. These results are helpful for a molecular-level understanding of the transformation of arsenic species, which in turn provides a theoretical foundation for the emission and control of arsenic.
Key words: CO; transformation of arsenic species; thermodynamic; kinetic; density functional theory

1. Introduction

Arsenic is a common element in coal, and all types of arsenic species are toxic except for the elemental form [1, 2]. Most of the arsenic in coal first evaporates in the flame zone during coal combustion. It subsequently, condenses on the surface of particulate matter as the flue gas cools down, and part of the arsenic finally escapes to the atmosphere [3-5]. Arsenic-bearing flue gas and solid waste from coal-fired power plants pose a serious problem for human health and the environment. Understanding the transformation of arsenic species during coal combustion will contribute much to the capture and disposal of arsenic via air pollution control devices.

In the coal combustion process, many flue gas arsenic species are possible [6-8]. In the research of Frandsen et al. [9], thermodynamic equilibrium calculations were performed to determine the transformation of arsenic species under different combustion atmospheres. It was found that AsO(g) is the stable species above 900K in an oxidizing atmosphere, while in a

Published by Elsevier. This is the Author Accepted Manuscript issued with: Creative Commons Attribution Non-Commercial No Derivatives License (CC:BY:NC:ND 4.0).
The final published version (version of record) is available online at DOI:10.1016/j.energy.2019.116024. Please refer to any applicable publisher terms of use.

Journal Pre-proof

reducing atmosphere, $As_2(g)$ is a probable species in the temperature range of 550K to 950K. As the temperature further increases AsO(g) is the only product. Contreras et al. [10] theoretically investigated the speciation of arsenic during oxy-fuel combustion, and found that $AsO_2(g)$ and AsO(g) are the most probable species at temperatures higher than 1073K. Miller et al. [11] studied the effect of HCl and SO_2 on the emission characteristics of arsenic during biomass combustion, and found that there are several possible species in the flue gas, such as AsO(g), $AsO_2(g)$. Chen et al. [12] and Jadhav et al. [13] pointed out that $As_2O_3(g)$ is the most common form of arsenic oxide. However, while the transformation of arsenic compounds has been studied in detail by means of thermodynamic equilibrium calculations, the kinetics of such transformations have been largely neglected.

Once released from coal, gaseous arsenic can react with other gas components in the flue gas. Urban and Wilcox [14] studied the reaction path of As and hydrogen chloride employing density functional theory and a broad range of *ab initio* methods, and the reaction rate constant was calculated by means of conventional transition state theory (TST) and collision theory. The research of Monahan-Pendergast et al. [15] predicted the arsenic species under atmospheric conditions by means of theoretical calculations, and possible reaction mechanisms of gaseous arsenic and radical species (OH, HO_2) were obtained. In our previous work, the reactions between As and nitrogen oxides were studied by density functional theory, and kinetic analysis was conducted to further elucidate the reaction mechanisms [16]. These studies showed that the transformation behavior of arsenic can be influenced significantly by the flue gas components.

Oxy-fuel combustion is considered to be an important technology for controlling anthropogenic CO_2 emissions [17-19]. During oxy-fuel combustion, thee are high concentration of CO_2 present which can react with char to produce a high concentration of CO [20, 21], which is strongly reducing [22]. Many researchers have studied the release and transformation of arsenic during oxy-fuel combustion [23-25], and pointed out that any refractory arsenic oxide would be reduced to the sub-oxides in a reducing atmosphere [26]. Experimentally, Zou et al. [27] investigated the volatilization characteristics of arsenic during isothermal oxy-fuel combustion, and found that the release of arsenic was suppressed compared to that in air combustion. The reason for this behavior is that CO generated by gasification between CO_2 and char affects the release and transformation of arsenic. However, the reaction mechanism between CO and arsenic oxides is unclear at present. Unfortunately, further understanding is limited by current arsenic measuring methods and it is difficult to experimentally investigate the reaction mechanism. Quantum chemistry offers a reliable method to study the reaction mechanism [28, 29], in order to gain a better understanding of the release behavior of arsenic oxides during coal combustion.

To date, recent experimental work has, in a preliminary fashion, explored the transformation characteristics of arsenic and pointed out that CO shows a strong reducing effect on arsenic oxides. However, the transformation mechanism for arsenic have not been developed to a satisfactory level due to a lack of theoretical calculations. Therefore, in this work, two typical arsenic oxide species, $AsO_2(g)$ and $As_2O_3(g)$ were employed to study the effect of CO on the transformation of arsenic species using density functional theory (DFT). Thermodynamic and kinetic parameters were analyzed to further study the reaction mechanism and the Multiwfn wavefunction analysis program [30] elucidated the relation between the reaction properties and electronic structures.

2. Computational methods

Density functional theory is widely used to study chemical reaction mechanisms because of its high accuracy and efficiency [31]. The choice of calculation method and basis set determines the computational efficiency and accuracy. B3LYP/6-31G(d) has been confirmed to be a good option for geometry optimizations [32]. Thus, in this work, geometry optimizations and frequency calculations of reactants, intermediates, transition states and products for each reaction were conducted with the B3LYP method in conjunction with the 6-31G(d) basis set. The values of frequency are all positive for reactants, intermediates and products, while there is only one negative value (imaginary frequency) for a transition state. Moreover, the intrinsic reaction coordinate (IRC) was calculated to confirm the transition state which connects the reactants and products. To obtain a more accurate result for energy, the single-point energy of each structure was calculated at the B2PLYP/Def2-TZVP level [33]. The zero-point energy (ZPE), obtained by frequency calculation, was used to revise the energy of each structure. All calculations in this work were performed by the Gaussian 16 software package [34], which can be used to study the molecular properties, including energy and structure of molecules, molecular orbitals, dipole moment, multipole moment, atomic charge, vibration frequency, Raman spectra, thermodynamic properties, reaction paths, etc.

The reaction rate constants were calculated at 298.15-1800K via the conventional transition state theory [35], and the formula is as follows:

$$k = k_T \times \frac{k_B T}{h} \times \frac{Q_{TS}}{Q_A Q_B} \times \exp(\frac{-E_a}{RT}) \qquad (1)$$

where k_T is the Wigner tunneling correction factor; k_B is the Boltzmann constant, $J \cdot K^{-1}$; h is the Planck constant, J·s; Q_{TS} is the partial function of the transition state; Q_A and Q_B are the partial functions of reactants A and B, respectively; E_a is the activation energy, $kJ \cdot mol^{-1}$; R is the molar gas constant, $J \cdot mol^{-1} \cdot K^{-1}$; and T is the thermodynamic temperature, K. The tunneling correction factor is calculated as follows:

$$k_T = 1 + (\frac{1}{24}) \times (\frac{h\nu_m c}{k_B T})^2 \qquad (2)$$

Here, ν_m accounts for the imaginary frequency of the transition state, cm^{-1}; and c is the velocity of light, $m \cdot s^{-1}$.

The equilibrium constant is calculated by the following formula [36]:

$$\Delta G = G_B - G_A = -RT \ln K \qquad (3)$$

where G_A and G_B are the Gibbs free energy of reactants and products, respectively, $kJ \cdot mol^{-1}$; and K is the equilibrium constant.

3. Results and discussion

3.1. Homogeneous reaction

Fig. 1 shows the homogeneous reaction process of CO and arsenic oxides (AsO_2 and As_2O_3); the major bond lengths and angles of reactants, intermediates, transition states and products are listed.

Journal Pre-proof

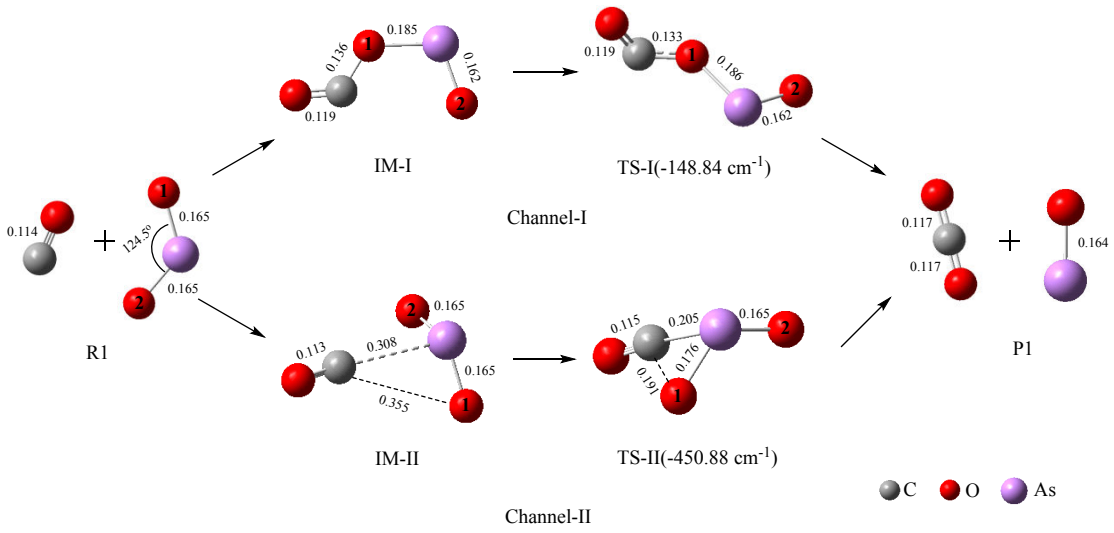

(a) Homogeneous reaction between AsO_2 and CO

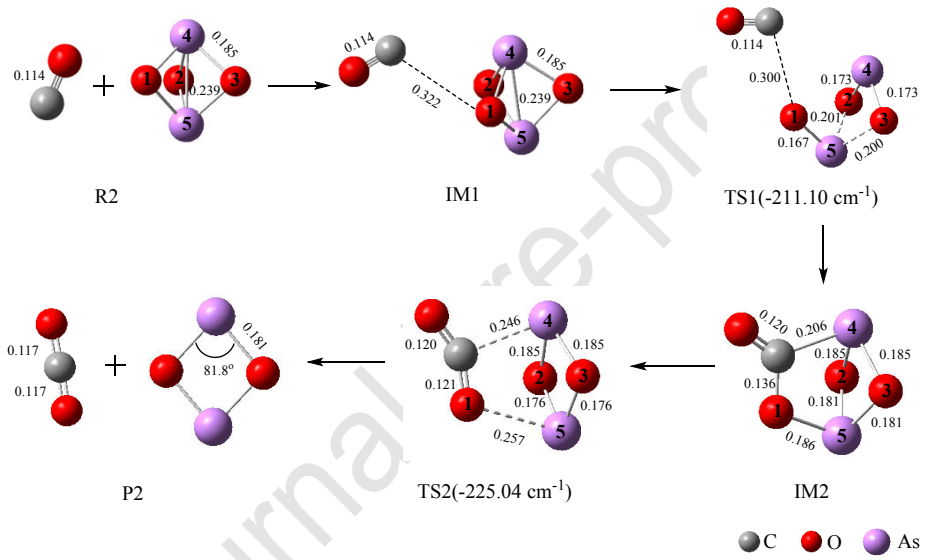

(b) Homogeneous reaction between As_2O_3 and CO

Fig. 1. Diagram of reaction between arsenic oxides and CO. The numbers are the bond lengths in nm.

Fig. 1(a) shows that there are two channels for the reaction of AsO_2 and CO. An intermediate and a transition state were found in each channel. For channel I, the C atom of CO is attached to the O(1) atom of AsO_2, forming the intermediate IM-I, then IM-I breaks down into AsO and CO_2 through the transition state TS-I. In this reaction process, the distance between the C atom of CO and the O(1) atom of AsO_2 decreases gradually (∞→0.136 nm→0.133 nm→0.117 nm, where ∞ means that the distance exceeds the bonding range), and the distance between As and O(1) increases gradually (0.165 nm→0.185 nm→0.186 nm→∞). For channel II, a CO molecule approaches the AsO_2 and forms the intermediate IM-II. There is a trend that the C atom gets close to the O(1) atom of AsO_2 as the distance between the two molecules decreases gradually. Subsequently, the IM-II undergoes an oxygen transfer and forms the AsO and CO_2 via the transition state TS-II.

In Fig. 1(b), the homogeneous reaction between As_2O_3 and CO is more complicated compared with the reaction between AsO_2 and CO. There are two transition states and two intermediates in the reaction process and, finally, As_2O_3 is reduced to the sub-oxides by CO. First,

CO is close to As_2O_3 and IM1 forms, and the distance between the C atom of CO and the O(1) atom of As_2O_3 decreases gradually as: ∞(R)→0.322 nm (IM1)→0.300 nm (TS1)→0.136 nm (IM2). A ring structure of IM2 is formed due to the combination of C-O(1) and C-As(4) bonds. Afterwards, with the rupture of C-As(4) and O(1)-As(5) bonds, IM2 transforms into CO_2 and As_2O_2.

Table 1 lists the calculated geometries of reactants and products at B3LYP/6-31G(d), and available experimental values, which shows that the B3LYP theoretical level along with the 6-31G(d) basis set is a favorable method for calculating structural properties.

Table 1. Calculated and experimental bond lengths (in nm) and bond angles (in deg)

Species	Bond length (r, nm) Bond angle (θ, deg)	Calculated	Experimental
CO	r(C-O)	0.114	0.113 [37]
AsO_2	r(As-O)	0.165	0.172 [38]
	θ(As-O-As)	124.5	122.2 [38]
AsO	r(As-O)	0.164	0.162 [15]
CO_2	r(C-O)	0.117	0.116 [37]
	θ(O-C-O)	180.0	180.0 [37]
As_2O_3	r(As-O)	0.185	0.184 [39]
	r(As-As)	0.239	0.238 [39]
As_2O_2	r(As-O)	0.181	0.187 [38]
	θ(O-As-O)	81.8	79.5 [38]

The energies of each stationary structure relative to the reactants for the homogeneous reactions are shown in Fig. 2.

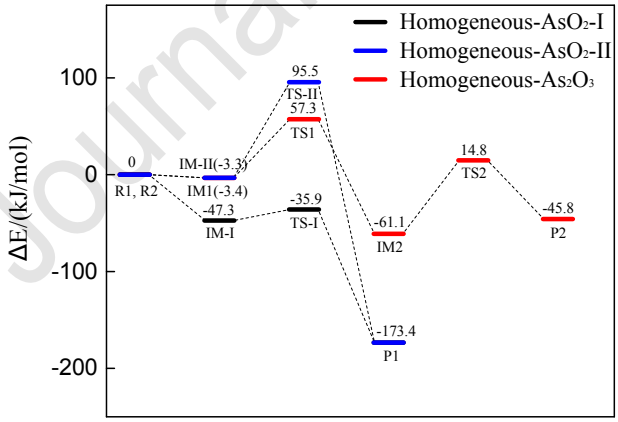

Fig. 2. Surface potential energy of the homogeneous reactions.

According to the transition state theory, activation energy is defined as the energy difference between transition state and reactant (or intermediate). As shown in Fig. 2, the activation energies of the homogeneous reaction between AsO_2 and CO are 11.4 kJ·mol^{-1} (for channel I) and 98.8 kJ·mol^{-1} (for channel II), respectively. These values show that AsO_2 and CO tend to form the intermediate IM-I, and finally generate AsO and CO_2. For the homogeneous reaction between As_2O_3 and CO, there are two transition states. The energy barrier is 60.7 kJ·mol^{-1} for the process

of IM1→IM2, and 75.9 kJ·mol^{-1} for the process of IM2→P2, indicating that the disengagement of CO_2 is the rate-determining step for the homogeneous reaction.

3.2. Heterogeneous reaction

In the process of coal combustion, gaseous arsenic tends to condense on fly ash particles as the temperature decreases [5]. Fly ash consists mainly of metal oxides and some unburned carbon, which serves as a good sorbent for gaseous arsenic [40]. Many researchers used char models to study heterogeneous reaction, and have found that char can provide active sites for reaction [21, 28, 32].

3.2.1. Model of char surface

In general, the carbonaceous surface is modeled by a single-layer graphite structure composed of several benzene rings, for which zigzag carbon bonding is an ideal model for quantum computation [41, 42]. Zhou et al. [43] studied the heterogeneous reduction mechanism of NO by the zigzag carbon bond model. In addition, the zigzag model has been employed to study the adsorption of hazardous elements by many other researchers [40, 44, 45]. Thus, the zigzag model with five benzene rings was chosen to explore the effect of CO on the transformation of arsenic species in this work. The char model is shown in Fig. 3.

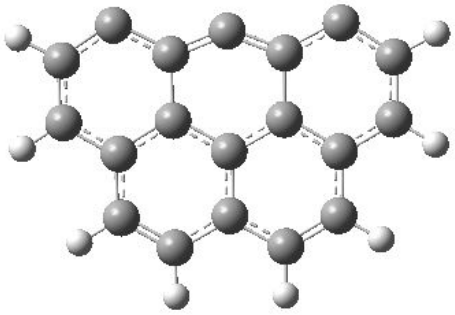

Fig. 3. Model of char surface.

On the char surface, three unsaturated C atoms on the upper side act as the active sites, and other C atoms at the edge are terminated with H atoms. All atoms of the model are coplanar, showing that the carbonaceous surface is modeled by a single-layer graphite structure. In this model, the average C-C bond length is 0.141 nm, and the average C-H bond length is 0.109 nm. These calculation results are close to the values reported in previous research [41], which indicates that the model here is reasonable.

3.2.2. Reaction process

The optimized structures of reactants, intermediates, transition states and products during the heterogeneous reactions of arsenic oxides (AsO_2 and As_2O_3) with CO are presented in Fig. 4, and the major bond lengths and angles of each molecular structure are given.

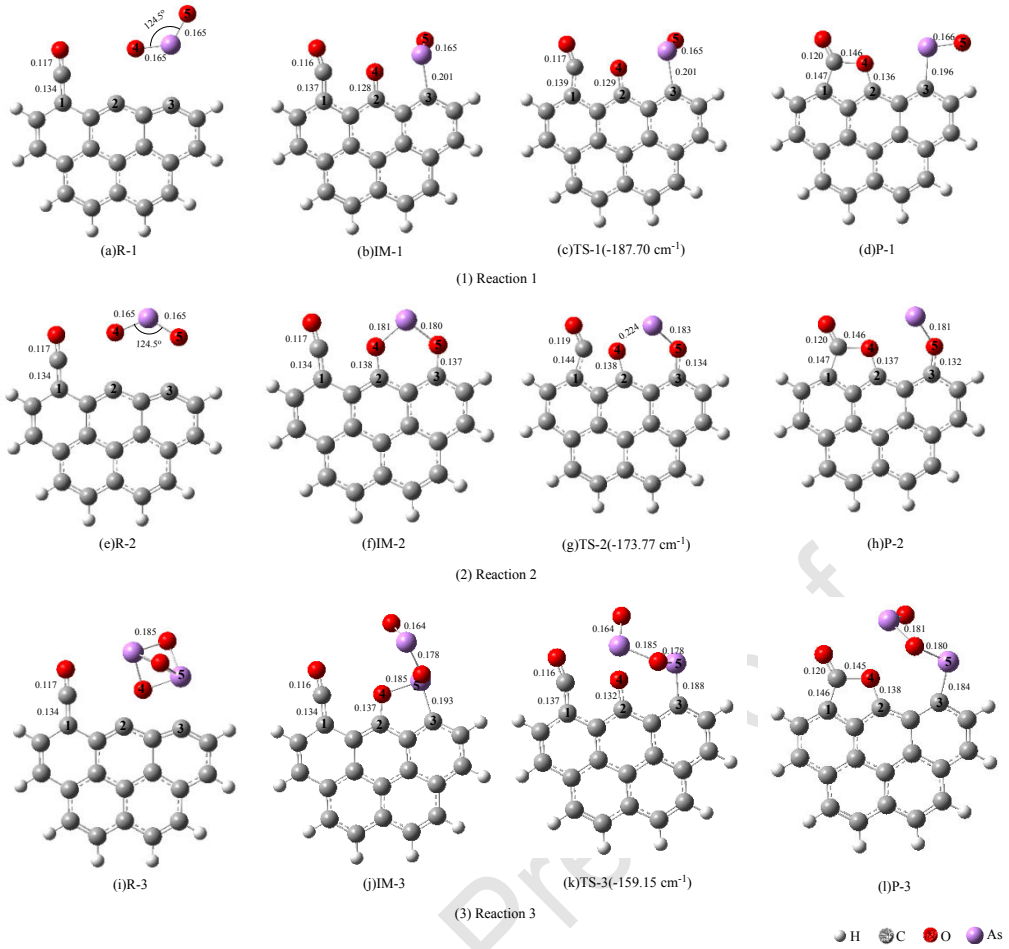

Fig. 4. Optimized structures for the heterogeneous reaction process. The numbers are the bond lengths in nm.

For reaction 1, the As atom and the O(4) atom of AsO_2 molecule are close to the char surface, and form O(4)-C(2) and As-C(3) bonds. The O(4) atom gradually approaches the C atom of CO, and finally forms the product (P-1). For reaction 2, a six-membered ring forms as the two O atoms of the AsO_2 molecule are attached to the surface of char. Subsequently, the ring structure breaks, and the length of the As-O(4) bond increases from 0.181 nm (IM-2) to 0.224 nm (TS-2). Fig. 4, shows that the products of reaction 1 and 2, P-1 and P-2 are CO_2 and AsO absorbed on the char surface. At the same time, the As-C(3) bond forms in P-1, and O(5)-C(3) bond in P-2. The reason is that the adsorption mode of the AsO_2 molecule on the char surface is different between R-1 and R-2. For reaction 3, an As_2O_3 molecule is absorbed on the char, becoming the intermediate IM-3 with a five-membered ring. There is a trend of the O(4) atom of As_2O_3 on the char surface associating with the C atom of CO as the distance gradually decreases. Finally, the intermediate IM-3 transfers into P-3 across the transition state TS-3.

The energies of each stationary structure relative to the reactants for the heterogeneous reactions are presented in Fig. 5.

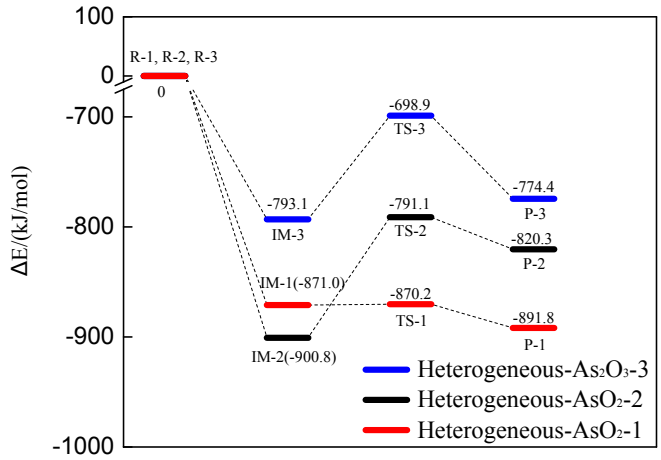

Fig. 5. Surface potential energy of the heterogeneous reactions.

Fig. 5 shows that an AsO_2 or As_2O_3 molecule is adsorbed on the surface of char, and the intermediates (IM-1, IM-2, and IM-3) are formed with a decrease of energy. According to adsorption theory, the adsorption energy (E_{ads}) is defined as the energy difference between the system before and after adsorption [46]. A reaction is divided into physical absorption (-30~-10 kJ·mol^{-1}) and chemical adsorption (-960~-50 kJ·mol^{-1}) according to the value of E_{ads} [40, 47, 48]. For the three heterogeneous reactions, the adsorption steps belong to chemical adsorption. The adsorption energy for the As_2O_3 molecule is 793.1 kJ·mol^{-1} during the R-3→IM-3 process. The energy of intermediate IM-2 (-900.8 kJ·mol^{-1}) is lower than that of IM-1 (-871.0 kJ·mol^{-1}), which indicates that the adsorption mode of AsO_2 molecule in reaction 2 is more stable.

For reaction 1, the activation energy of the process IM-1→P-1 is only 0.8 kJ·mol^{-1}, which means that this reaction takes place easily. The six-membered ring in IM-2 undergoes the dissociation of As-O(4) and the product P-2 (a five-membered ring) forms with the formation of the O(4)-C (the C atom of CO) bond. This process is endothermic and must overcome an energy barrier of 109.7 kJ·mol^{-1}. For reaction 3, the O(4) atom of As_2O_3 moves away from the As(5) and gradually approaches the C atom of CO. In this process, the intermediate IM-3 transforms into the product P-3 after crossing an energy barrier of 94.2 kJ·mol^{-1}.

3.3. Thermodynamic analysis

Thermodynamic parameters are helpful for further understanding the reaction process. Thermodynamic parameters of the homogeneous reaction between arsenic oxides (AsO_2 and As_2O_3) and CO are calculated at 298.15~1800 K, and results are listed in Table 2.

Table 2 Thermodynamic parameters at different temperatures

Temperature	AsO_2 and CO			As_2O_3 and CO		
(K)	ΔH, kJ·mol^{-1}	ΔS, J·mol^{-1}·K^{-1}	ΔG, kJ·mol^{-1}	ΔH, kJ·mol^{-1}	ΔS, J·mol^{-1}·K^{-1}	ΔG, kJ·mol^{-1}
298.15	-174.39	-106.38	-142.67	-47.15	-116.59	-12.38
600	-173.00	-103.35	-110.99	-47.81	-118.24	23.13
900	-170.64	-100.19	-80.47	-47.78	-118.21	58.62
1200	-167.77	-97.45	-50.83	-47.30	-117.77	94.02

1500	-164.62	-95.11	-21.96	-46.59	-117.24	129.27
1800	-161.31	-93.10	6.26	-45.73	-116.72	164.36

From Table 2, it can be found that the enthalpy difference (ΔH) of the homogeneous reactions between arsenic oxides (AsO_2 and As_2O_3) and CO are negative. This confirms that the homogeneous reduction reaction of arsenic oxides is an exothermic process. Moreover, the released heat of the AsO_2/CO reaction is about four times as large as that for the As_2O_3/CO reaction. The Gibbs free energy difference (ΔG) gradually increases from -142.67 to 6.26 kJ·mol^{-1} for the AsO_2 and CO reaction, and from -12.38 to 164.36 kJ·mol^{-1} for the As_2O_3 and CO reaction when the temperature rises from 298.15 K to 1800 K. According to the Gibbs free energy principle, ΔG<0 means that the reaction can occur spontaneously. Therefore, the "spontaneity" of AsO_2 and CO reaction decreases with increasing temperature, and the reaction cannot occur spontaneously over a certain temperature. As shown in Table 2, the values of ΔG are positive except for the -12.38 kJ·mol^{-1} value at 298.15 K for the As_2O_3 and CO reaction, suggesting that the reaction cannot take place spontaneously during coal combustion in a furnace.

In addition, the equilibrium constant is also an important thermodynamic parameter, which can determine the degree of the reaction. Equilibrium constants at different temperatures were calculated using the data of Table 2, and results are shown in Fig. 6.

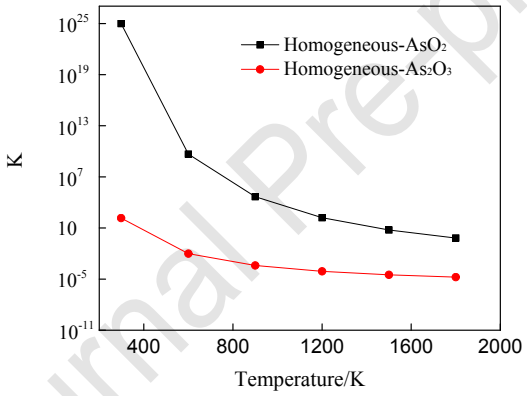

Fig. 6. Equilibrium constants at different temperatures.

In Fig. 6, it can be shown that the equilibrium constant decreases with temperature for the arsenic oxides (AsO_2 and As_2O_3) and CO reactions. For the AsO_2 and CO homogeneous reaction, the equilibrium constant is higher than 10^5 at a low temperature (about <900 K), indicating that the reaction process goes to completion and take place irreversibly [32]. With the increase of temperature, the degree of the chemical reaction is reduced and for the homogeneous reaction between As_2O_3 and CO, the equilibrium constant is always lower than 10^3 over the temperature range between 298.15~1800 K, suggesting that the reaction will not go to completion.

3.4. Kinetic analysis

Kinetic parameters, such as reaction rate constant, pre-exponential factor and activation energy, were calculated by the conventional transition state theory in the temperature range of 298.15-1800 K, as shown in Fig. 7.

Journal Pre-proof

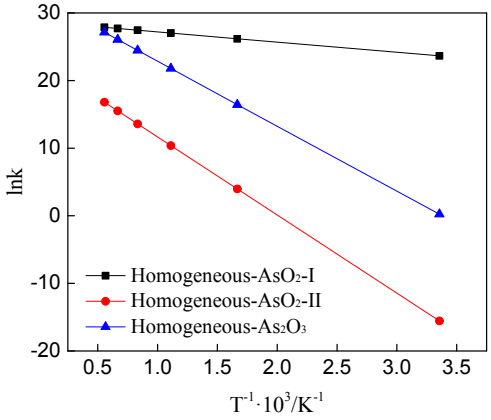

(a) Homogeneous reactions

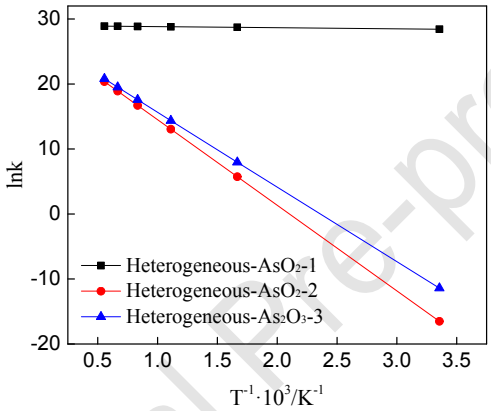

(b) Heterogeneous reactions

Fig. 7. Reaction rate constants of all rate-determining steps at 298.15 K-1800 K.

From Fig. 7, it can be seen that the reaction rate constants increase with temperature, and there is a strong linear relation between lnk and 1000/T for all reactions. Table 3 gives the pre-exponential factor and activation energy obtained from this data.

Table 3. Reaction kinetic parameters

Reaction	Pre-exponential factor A	Activation energy E_A (kJ·mol^{-1})	Arrhenius equation
Homogeneous-AsO_2-I	2.92×10^{12}	12.49	$k=2.92\times10^{12}\exp(-1502.52/T)$
Homogeneous-AsO_2-II	1.21×10^{10}	96.05	$k=1.21\times10^{10}\exp(-11552.8/T)$
Homogeneous-As_2O_3	1.26×10^{14}	79.89	$k=1.26\times10^{14}\exp(-9609.09/T)$
Heterogeneous-AsO_2-1	3.91×10^{12}	1.41	$k=3.91\times10^{12}\exp(-169.59/T)$
Heterogeneous-AsO_2-2	1.05×10^{12}	109.48	$k=1.05\times10^{12}\exp(-13168.15/T)$
Heterogeneous-As_2O_3-3	6.25×10^{11}	95.61	$k=6.25\times10^{11}\exp(-11499.88/T)$

As shown in Table 3, for the homogeneous reaction of AsO_2 and CO, the pre-exponential factor of channel I is two orders of magnitudes larger than that of channel II, and the activation energy of channel I is much lower than for channel II. This suggests that AsO_2 tends to react with CO via channel I. For the heterogeneous reaction of AsO_2 and CO, the activation energies of reaction 1 and reaction 2 are 1.41 kJ·mol^{-1} and 109.48 kJ·mol^{-1}, respectively, meaning that

compared with the homogeneous reaction of AsO_2 and CO, char has a positive effect on AsO_2 reduction for the heterogeneous reaction 1, while energy barrier of AsO_2 reduction would increase for the heterogeneous reaction 2. In addition, the activation energy of the As_2O_3 homogeneous reduction is lower than that of the heterogeneous reduction, indicating that As_2O_3 is more likely to react with CO in flue gas.

3.5. Electron density analysis

The essence of any chemical reaction is the rearrangement of atoms, including the transfer of electrons. Electron density differences of transition states for the reactions were calculated to explore the transfer of electrons during the reaction process, and the results are shown in Fig. 8.

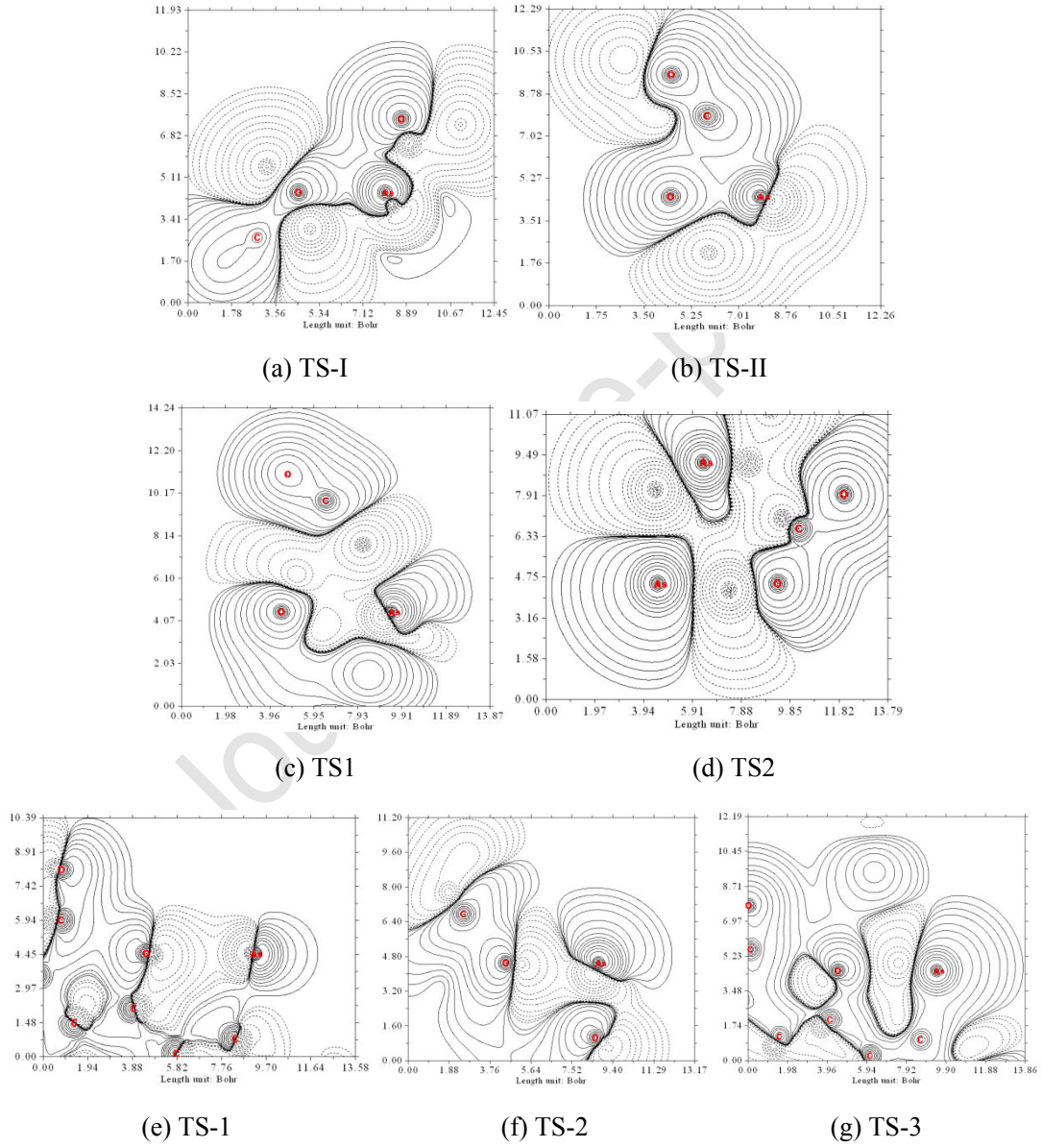

(a) TS-I (b) TS-II

(c) TS1 (d) TS2

(e) TS-1 (f) TS-2 (g) TS-3

Fig. 8. The contour maps of electron density differences of each transition state

In the graph, solid lines and dashed lines correspond to the regions where electron density is increased and decreased, respectively. The contour map of electron density clearly shows variation of electron density distribution for the reactions. For example, it shows that the electron density between O and As decreases while the electron density between O and C increases in Fig. 8(d). It

also shows that a stable chemical bond between an O atom of As_2O_3 and C atom would be formed to obtain a CO_2 molecule. This observation is in line with the homogeneous reaction mechanism of As_2O_3 and CO.

4. Conclusions

In recent years, numerous researchers have experimentally investigated the release and transformation characteristics of arsenic during coal combustion. However, little theoretical research effort has been made on arsenic behavior in the coal combustion process. To explore the transformation mechanism of arsenic, density functional theory (DFT) was employed to study the homogeneous and heterogeneous reaction processes of arsenic oxides (AsO_2 and As_2O_3) with CO. In addition, thermodynamic and kinetics parameters were calculated to reveal the reaction mechanism. The main conclusions are summarized as follows:

(1) There are two channels for the homogeneous reaction of AsO_2 and CO, and a transition state was found in each channel. The homogeneous reaction between As_2O_3 and CO undergoes two transition states and two intermediates, and finally As_2O_3 is reduced to the sub-oxides by CO.

(2) For the three heterogeneous reactions, char possesses a strong adsorption ability towards AsO_2 and As_2O_3 in the presence of CO, and the intermediates experience a transition state to generate the corresponding products.

(3) The adsorption mode of AsO_2 molecule on the char surface has a great influence on its reduction. The activation energy for the reaction of the two O atoms of the AsO_2 molecule being absorbed on the surface of char is 109.7 $kJ \cdot mol^{-1}$, while it is only 0.8 $kJ \cdot mol^{-1}$ for the reaction of the As atom and O atom of the AsO_2 molecule absorbed on the surface.

(4) The activation energy of the homogeneous reduction of As_2O_3 (75.9 $kJ \cdot mol^{-1}$) is lower than the heterogeneous reduction (94.2 $kJ \cdot mol^{-1}$), which suggests that As_2O_3 is more likely to react with CO in the flue gas.

Acknowledgement

The financial support from Fundamental Research Funds for the Central Universities (2018ZD03) and Key Research and Development (R&D) Projects of Shanxi Province (201803D31027) are gratefully acknowledged.

Nomenclature

AsO	arsenic monoxide
AsO_2	arsenic dioxide
As_2O_3	arsenic trioxide
TST	conventional transition state theory
CO_2	carbon dioxide
CO	carbon monoxide
DFT	density functional theory
IRC	intrinsic reaction coordinate
ZPE	zero-point energy

Journal Pre-proof

k	reaction rate constant
k_T	Wigner tunneling correction factor
k_B	Boltzmann constant ($J \cdot K^{-1}$)
h	Planck constant ($J \cdot s$)
Q_{TS}	partial function of transition state
Q_A	partial functions of reactant A
Q_B	partial functions of reactant B
E_a	the calculated DFT activation energy ($kJ \cdot mol^{-1}$)
R	molar gas constant ($J \cdot mol^{-1} \cdot K^{-1}$)
T	thermodynamic temperature (K)
v_m	imaginary frequency of the transition state (cm^{-1})
c	velocity of light ($m \cdot s^{-1}$)
K	equilibrium constant
ΔG	Gibbs free energy difference ($kJ \cdot mol^{-1}$)
G_A	Gibbs free energy of reactant A ($kJ \cdot mol^{-1}$)
G_B	Gibbs free energy of product B ($kJ \cdot mol^{-1}$)
P	product
TS	transition state
E_A	apparent activation energy ($kJ \cdot mol^{-1}$)
A	pre-exponential factor
ΔH	enthalpy difference ($kJ \cdot mol^{-1}$)
ΔS	entropy difference ($J \cdot mol^{-1} \cdot K^{-1}$)

References:

[1] Zhang W, Sun Q, Yang X. Thermal effects on arsenic emissions during coal combustion process. Sci Total Environ 2018; 612: 582-589.

[2] Wang C, Liu H, Zhang Y, Zou C, Anthony EJ. Review of arsenic behavior during coal combustion: Volatilization, transformation, emission and removal technologies. Prog Energ Combust 2018; 68: 1-28.

[3] Akira O, Tsunenori N, Yuka S, Akira I, Hirokazu T. Analysis of arsenic and some other elements in coal fly ash by X-ray photoelectron spectroscopy. J Hazard Mater 2005; 119: 213-217.

[4] Zhao Y, Zhang J, Huang W, Wang Z, Li Y, Song D, et al. Arsenic emission during combustion of high arsenic coals from Southwestern Guizhou, China. Energ Convers Manage 2008; 49: 615-624.

[5] Liu H, Wang C, Zou C, Zhang Y, Wang J. Simultaneous volatilization characteristics of arsenic and sulfur during isothermal coal combustion. Fuel 2017; 203: 152-161.

[6] Wang H, Duan Y, Li Y, Xue Y, Liu M. Prediction of synergic effects of H_2O, SO_2, and HCl on mercury and arsenic transformation under oxy-fuel combustion conditions. Energ Fuel 2016; 30: 8463-8468.

[7] Contreras ML, Arostegui JM, Armesto L. Arsenic interactions during co-combustion processes based on thermodynamic equilibrium calculations. Fuel 2009; 88: 539-546.

[8] Díaz-Somoano M, Unterberger S, Hein K. Prediction of trace element volatility during co-combustion processes. Fuel 2006; 85: 1087-1093.

[9] Flemming F, Kim R, Peter D. Trace elements from combustion and gasification of coal—An

Journal Pre-proof

equilibrium approach. Prog Energ Combust 1994; 20: 115-138.

[10] Contreras ML, García-Frutos FJ, Bahillo A. Oxy-fuel combustion effects on trace metals behaviour by equilibrium calculations. Fuel 2013; 108: 474-483.

[11] Miller B, Dugwell DR, Kandiyoti R. The Influence of Injected HCl and SO_2 on the Behavior of Trace Elements during Wood-Bark Combustion. Energy and Fuels 2003; 17: 1382-1391.

[12] Chen D, Hu H, Xu Z, Liu H, Cao J, Shen J, et al. Findings of proper temperatures for arsenic capture by CaO in the simulated flue gas with and without SO_2. Chem Eng J 2015; 267: 201-206.

[13] Jadhav RA, Fan L. Capture of gas-phase arsenic oxide by lime: Kinetic and mechanistic studies. Environ Sci Technol 2001; 35: 794-799.

[14] Urban DR, Wilcox J. Theoretical study of the kinetics of the reactions $Se + O_2 \rightarrow Se + O$ and $As + HCl \rightarrow AsCl + H$. J Phys Chem a 2006; 110: 8797-8801.

[15] Monahan-Pendergast M, Przybylek M, Lindblad M, Wilcox J. Theoretical predictions of arsenic and selenium species under atmospheric conditions. Atmos Environ 2008; 42: 2349-2357.

[16] Zou C, Wang C. Theoretical study of the reactions between arsenic and nitrogen oxides during coal combustion. J Mol Model 2019; 25.

[17] Gładysz P, Stanek W, Czarnowska L, Sładek S, Szlęk A. Thermo-ecological evaluation of an integrated MILD oxy-fuel combustion power plant with CO_2 capture, utilisation, and storage – A case study in Poland. Energy 2018; 144: 379-392.

[18] Gładysz P, Ziębik A. Life cycle assessment of an integrated oxy-fuel combustion power plant with CO_2 capture, transport and storage – Poland case study. Energy 2015; 92: 328-340.

[19] Gopan A, Kumfer BM, Phillips J, Thimsen D, Smith R, Axelbaum RL. Process design and performance analysis of a staged, pressurized oxy-combustion (SPOC) power plant for carbon capture. Appl Energ 2014; 125: 179-188.

[20] Hecht ES, Shaddix CR, Geier M, Molina A, Haynes BS. Effect of CO_2 and steam gasification reactions on the oxy-combustion of pulverized coal char. Combust Flame 2012; 159: 3437-3447.

[21] Jiao A, Zhang H, Liu J, Jiang X. Quantum chemical and kinetics calculations for the NO reduction with char(N): Influence of the carbon monoxide. Combust Flame 2018; 196: 377-385.

[22] Jiao A, Zhang H, Liu J, Shen J, Jiang X. The role of CO played in the nitric oxide heterogeneous reduction: A quantum chemistry study. Energy 2017; 141: 1538-1546.

[23] Liu H, Wang C, Sun X, Zhang Y, Zou C. Volatilization of arsenic in coal during isothermal oxy-fuel combustion. Energ Fuel 2016; 30: 3479-3487.

[24] Wang C, Liu X, Li D, Wu W, Xu Y, Si J, et al. Effect of H_2O and SO_2 on the distribution characteristics of trace elements in particulate matter at high temperature under oxy-fuel combustion. Int J Greenh Gas Con 2014; 23: 51-60.

[25] Roy B, Bhattacharya S. Release behavior of Hg, Se, Cr and As during oxy-fuel combustion using Loy Yang brown coal in a bench-scale fluidized bed unit. Powder Technol 2016; 302: 328-332.

[26] Quann RJ, Sarofim AF. Vaporization of refractory oxides during pulverized coal combustion. Symposium (International) on Combustion 1982; 19: 1429-1440.

[27] Zou C, Wang C, Liu H, Wang H, Zhang Y. Effect of volatile and ash contents in coal on the volatilization of arsenic during isothermal coal combustion. Energ Fuel 2017; 31: 12831-12838.

[28] Zhang H, Liu J, Shen J, Jiang X. Thermodynamic and kinetic evaluation of the reaction between NO (nitric oxide) and char(N) (char bound nitrogen) in coal combustion. Energy 2015; 82: 312-321.

[29] Liu J, Qu W, Yuan J, Wang S, Qiu J, Zheng C. Theoretical studies of properties and reactions

involving mercury species present in combustion flue gases. Energy and Fuels 2010; 24: 117-122.

[30] Lu T, Chen F. Multiwfn: A multifunctional wavefunction analyzer. J Comput Chem 2012; 33: 580-592.

[31] Arkan F, Izadyar M, Nakhaeipour A. The role of the electronic structure and solvent in the dye-sensitized solar cells based on Zn-porphyrins: theoretical study. Energy 2016; 114: 559-567.

[32] Gao Z, Yang W, Ding X, Ding Y, Yan W. Theoretical research on heterogeneous reduction of N_2O by char. Appl Therm Eng 2017; 126: 28-36.

[33] Padma MEJ, Divya P. Structural stability in dimer and tetramer clusters of L-alanine in the gas-phase and the feasibility of peptide bond formation. The journal of physical chemistry. B 2018.

[34] Frisch MJ, Trucks GW, Schlegel HB, Scuseria GE, Robb MA, Cheeseman JR, et al. Gaussian, Inc., Wallingford CT. 2016.

[35] Bravo-Perez G, Alvarez-Idaboy JR, Cruz-Torres A, Ruiz ME. Quantum chemical and conventional transition-state theory calculations of rate constants for the NO_3 plus alkane reaction. J Phys Chem a 2002; 106: 4645-4650.

[36] Korevaar PA, George SJ, Markvoort AJ, Smulders MMJ, Hilbers PAJ, Schenning APHJ, et al. Pathway complexity in supramolecular polymerization. Nature 2012; 481: 492-496.

[37] Hu C, Hu H, Li M, Tian A. Comparative study of the interaction of CO and CO_2 with Ni_2 cluster. Journal of Molecular Structure: Theochem 1999; 491: 155-160.

[38] Rosli AN, Zabidi NA, Kassim HA, Shrivastava KN. Ab initio calculation of vibrational frequencies of AsO glass. J Non-Cryst Solids 2010; 356: 428-433.

[39] Da Hora GCA, Longo RL, Da Silva JBP. Calculations of structures and reaction energy profiles of As2O3 and As4O6 species by quantum chemical methods. Int J Quantum Chem 2012: 3320-3324.

[40] Gao Z, Li M, Sun Y, Yang W. Effects of oxygen functional complexes on arsenic adsorption over carbonaceous surface. J Hazard Mater 2018; 360: 436-444.

[41] Yang FH, Yang RT. Ab initio molecular orbital study of adsorption of atomic hydrogen on graphite: Insight into hydrogen storage in carbon nanotubes. Carbon 2002; 40: 437-444.

[42] Ning C, Yang RT. Ab initio molecular orbital calculation on graphite: selection of molecular system and model chemistry. Carbon 1998; 36: 1061-1070.

[43] Zhou Z, Zhang X, Zhou J, Liu J, Cen K. A molecular modeling study of N_2 desorption from NO heterogeneous reduction on char. Energy Sources Part A: Recovery, Utilization and Environmental Effects 2014; 36: 158-166.

[44] Liu J, Qu W, Zheng C. Theoretical studies of mercury–bromine species adsorption mechanism on carbonaceous surface. P Combust Inst 2013; 34: 2811-2819.

[45] Liu J, Cheney MA, Wu F, Li M. Effects of chemical functional groups on elemental mercury adsorption on carbonaceous surfaces. J Hazard Mater 2011; 186: 108-113.

[46] Amaya-Roncancio S, Garcia Blanco AA, Linares DH. DFT study of hydrogen adsorption on Ni/graphene. Appl Surf Sci 2018; 447: 254-260.

[47] Gao Z, Yang W. Effects of CO/CO_2/NO on elemental lead adsorption on carbonaceous surfaces. Journal Molecular Modeling 2016; 22: 166.

[48] Guo X, Zhao P, Zheng C. Theoretical study of different speciation of mercury adsorption on CaO (0 0 1) surface. P Combust Inst 2009; 32: 2693-2699.

Journal Pre-proof

There are no conflicts of interest.

Journal Pre-proof

Journal Pre-proof

Highlights

Reaction mechanism of homogeneous and heterogeneous reactions of arsenic oxides with CO were revealed via density functional theory.

The adsorption mode of AsO_2 molecule on the char surface has a great influence on its reduction.

As_2O_3 homogeneous reduction with CO is more likely to take place compared to the heterogeneous reduction.

Journal Pre-proof

https://dspace.org/

The effect of CO on the transformation of arsenic species: A quantum chemistry study

Anthony, Edward J.; Zou, Chan

2020-08-27
Elsevier
https://doi.org/10.1016/j.energy.2019.116024
Zou C, Wang C, Anthony E. (2019) The effect of CO on the transformation of arsenic species: a quantum chemistry study. Energy, Volume 187, November 2019, Article number 116024

Downloaded from a DSpace repository. https://dspace.org/